Aerodynamic Simulation of a Blimp Kind Unmanned Aerial Vehicle for Stable Environmental Conditions

J. A. López, L. A. Aguilera, M. Ponce, L. Basaca
CETYS Universidad, Ensenada, México.
Email: Josue.lopez@cetys.mx

R. I. Ramos Garcia
Phyn LLC Data Sciencie & Mchine Learning, Seatle, USA,
Email: raul.ramos@phyn.com

V.M Ramos Garcia
University of Sonora, Navojoa, Mexico
Email: victor.ramos@navojoa.uson.mx

***Abstract*—An Unmanned Aerial Vehicle blimp kind prototype for stable environmental conditions is shown in this paper. The lift, drag, weight, and thrust parameters are analyzed on the basis of the Archimedes principle, Bernoulli and continuity equations, and fluid simulations for different conditions (low-speed wind and absence of turbulence). The calculated push force (lift) is the minimum value to produce sustentation considering the overall mass of the aircraft. On the other hand, the drag parameter was analyzed using the fluid simulation to visualize the drag force.**

***Index Terms*—lift, drag, fluid simulation, unmanned aerial vehicle.**

I. Introduction

Unmanned Aerial Vehicles (UAVs) are an effective way to inspect, document, and search, among other similar actions in different topologies [1, 3]. Generally speaking, UAVs are equipped with different data-acquisition systems that can be used from heights up to 800 m [4]. With these characteristics, UAVs provide certain advantages, such as effective pinpointing of certain places within a range of 10 km^2 and providing aerial security when the field is unstable and unsecure, while also being less expensive than a LIDAR, among others [5]. Specifically, a blimp kind UAV (i.e., Zeppelin) is highly useful for an application with reduced mass and speed. However, important design aspects with respect to aerodynamic parameters, such as envelopes, stabilizers, rudder systems, envelope pressurization, load distribution (and load-taking systems) in normal conditions, or well-calibrated simulations (tunnel winds), have to be considered [6, 7]. There are different aspects that modify the performance, such as aerostatic parameters, heat distribution, and quality of the wrapping materials. Consequently, the complete design of a UAV requires three phases: conceptual design, preliminary design, and detailed design. Naturally, there are more phases once the manufacturing process is initiated. In particular, the first phase is ideal to adjust parameter modeling and initial tests with the purpose of improving, or modifying, the generic structure of the UAV [8]. An important parameter in the aerodynamic context is the "lift-induced drag," which defines the horizontal component (drag, D) of the reaction force in the UAV; it must also be minimized in the elevation process (lift, L). In addition, there are various parameters that affect the drag in a UAV; these are called parasitic drag (D_p) [9, 10]. In this paper, the conceptual design of a UAV type Zeppelin is shown, among some aerodynamic measurements of the elevation, parameters, dragging conditions, weight, and thrust under controlled atmospheric conditions. This paper is organized as follows. Section II gives a brief description of the conceptual design and components used, the mathematical background is shown in Section III, and, finally, Section IV shows the visual simulation results of the UAV regarding the lift, drag, weight, and thrust parameters.

II. General Conceptual Design and Components

The proposed UAV is shown in Fig. 1. In particular, a dirigible gondola (without the globe or wrapping) and its three electrical motors shown; centrally aligned to the axis of the gondola are the ones that will give horizontal flight to the UAV (related to the thrust and drag). The third motor, located underneath the gondola, is used to control the takeoff and landing (related to the lift and weight). The main support of the dirigible is a globe with helium, which is sustained on the basis of the Archimedes principle [11]; thus, control landing will be operated or controlled by means of the third motor. The conceptual design establishes that the total load of the UAV is slightly more than the support that the globe manages to create and keep the UAV on stable earth, so the application of slight propulsion to the third motor, the UAV, will rise. However, this action considers that the

Manuscript received November 6, 2017; revised February 1, 2018.

doi: 10.18178/ijmerr.7.2.197-201

electric current is lower than other actions for the propulsion; therefore, an energy saving is made to increase flying time.

Figure 1. Gondola design considering motor positions and helixes or propellers (frontal view) [12].

The electrical controller setup for the UAV is shown in Figs. 2 and 3, with the purpose of calculating the center of mass. Table I shows the specific mass of each electronic component used.

TABLE I. SPECIFIC COMPONENT MASS.

Electronic component	Mass (g)
Brushless motor A2213/13T (x3)	141
BLDC ESC 30 A (x3)	66
BeagleBone Black	40
Wi-Fi/Bluetooth USB adapter	10
9-volt battery (x3)	190
Lipo Multistar battery 5,200 mAh	450
Electronics (voltage regulators and cables)	20

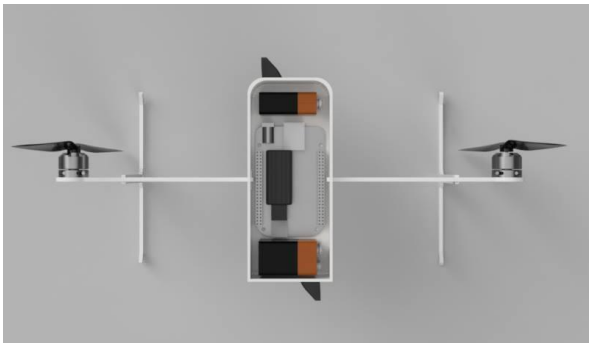

Figure 2. Gondola design and motors' positions (superior view) [12].

Figure 3. Gondola design and motors' positions (lateral view) [12].

To obtain the sustentation of the UAV, an aerostatic globe was acquired. Once the dimensions of the inflated globe were known, a Computer-Aided Design (CAD) was made just as shown in Fig. 4.

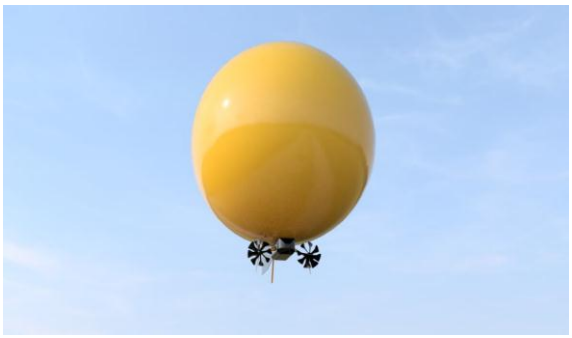

Figure 4. CAD of the overall UAV [12].

III. MATHEMATICAL BACKGROUND

The masses of the electronic elements mentioned in Table I were considered; using 3D printing software, it was determined whether the mass (in relationship with the weight) of these could be supported with the acquired globe. To calculate the required support strength of the prototype, the Archimedes principle and Bernoulli equation were used. In this case, filling the globe with helium creates a differential pressure with respect to the air; for this, the air density D_{air} and helium D_{He} were used as follows:

$$D_{\text{air}} = 1.19 \text{ kg/m}^3, \quad (1)$$

$$D_{\text{He}} = 0.18 \text{ kg/m}^3. \quad (2)$$

Next, the corresponding weight is calculated, meaning:

$$P_{\text{air}} = gD_{\text{air}} = 11.67 \text{ kg/m}^2\text{s}^2, \quad (3)$$

$$P_{\text{He}} = gD_{\text{He}} = 1.765 \text{ kg/m}^2\text{s}^2. \quad (4)$$

Afterwards, the displaced volume (V) was calculated as per the globe, where $V = 0.94867 \text{ m}^3$. Based on the latter, the upward push force (lift) is calculated:

$$F = V(P_{\text{air}} - P_{\text{He}}) - 0.035\, gKg = 9.053 \text{ N}. \quad (5)$$

The F value is equal to the difference of the specific gas weight multiplied by the displaced volume, subtracting the weight of the globe. In consequence, F is divided by the gravity, and the weight that can lift the glove is calculated as follows:

$$F_{\text{asc}} = \frac{F}{g} = 0.923 \text{ kg}. \quad (6)$$

In a particular way, the calculated weight cannot be overcome; if the load exceeds it, there will be no lift. The drag (D) can be expressed as $D = \left(\rho {V_a}^2 C_D S\right)/2$, where ρ is the air density, V_a is the airspeed, C_D is a nondimensional drag coefficient, and S is the frontal aircraft area. In our case, the value parameters are constant because of the particular application. On the

other hand, the horizontal thrust (the vertical thrust is related to the lift and weight, finally, meaning the vertical force F_v) of the UAV is defined as

$$T - \cos(\varphi) - D = F_h, \quad (7)$$

where φ is the angle between the horizontal axes of the UAV and the propulsion direction due to the propellers. The value of T due to the use of propellers is

$$T = [\rho A(V_{ae}^2 - V_{a0}^2)]/2, \quad (8)$$

where A is the propeller disk area and V_{ae} and V_{a0} are the velocity of air in the exit and the aircraft, respectively.

IV. Simulations

In this section, some simulation results are shown, using the 1.0 design version. The design and adequate propeller for the prototype were obtained using the *flow simulation tool* of the software SolidWorks. For the simulation, we considered a controlled atmosphere with winds of 0.5 m/s in the *y*-axis and a propeller speed of 25 rad/s with 5,000 rpm per motor. Due to the dirigible being for closed space, those considerations were taken, so that the air current and pressure are almost negligible.

Figure 5 shows how part of the circulating air in the *y*-axis is absorbed by the propeller, which fulfills its purpose of increasing its fluid velocity to generate horizontal propulsion to the prototype. Furthermore, in Fig. 6, only the air in the propellers is being isolated, which functions as a backup argument of what was mentioned beforehand. In particular, the maximum air flow speed is ≈ 0.05 m/s at the propeller's rear in comparison with ≈0.01 m/s at the propeller's entrance.

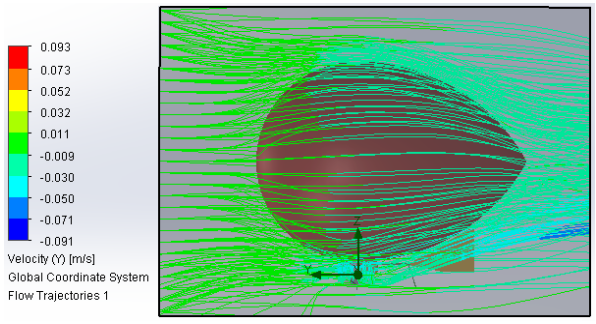

Figure 5. Fluid simulation on the *y*-axis; it is able to appreciate in blue color the change of speed due to the helix movement [12].

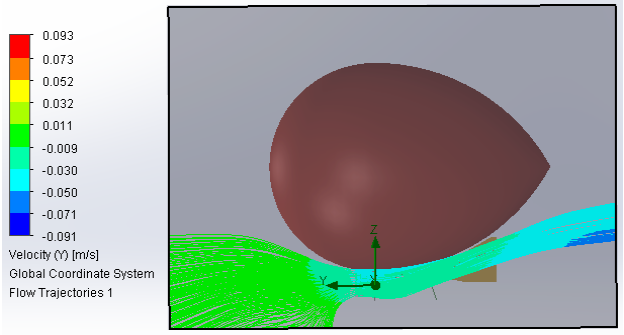

Figure 6. Air flow simulation only toward the helixes [12].

With the objective of obtaining complementary results for the prototype behavior simulation to improve the overall performance, the wind direction parameter was modified. Thus, this helps observe the aerodynamic efficiency from different angles, and it also helps in the observation and behavior analysis of the propellers that receive air from different angles.

In particular, Fig. 7 shows the air flow through the *z*-axis with the same speed (0.5 m/s), where it can be observed that the air flows softly through the prototype. When the propeller works, specifically at 25 rad/s, it absorbs the air that comes from underneath and generates small propulsion, pushing the air toward the *y*-axis, which modifies the lift and drag of the prototype.

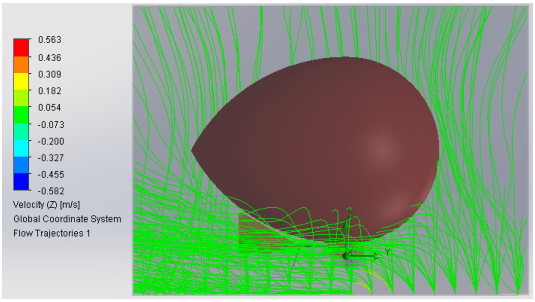

Figure 7. Upward wind ascension on the *z*-axis [12].

Another simulation was developed, which describes the air flowing on the *x*-axis with the same configuration of 0.5 m/s and turning speed of the helixes of 25 rad/s (see Fig. 8). It is seen that, on this axis, a weaker air flow is obtained, which is due to the geometry of the model and due to the propellers that generate a force that prevents the air from circulating in a laminated way through this axis, creating turbulences, or vortexes, when crashing with the prototype.

Figure 8 shows the behavior of the complete system, taking into consideration perpendicular wind, which does not significantly affect the aerodynamics. The dynamic behavior of the airflow in the propeller is also observable.

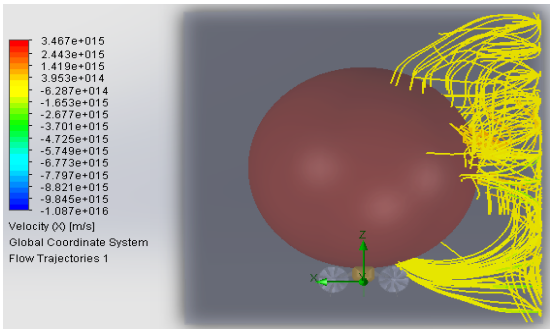

Figure 8. Simulation of the perpendicular wind toward the dirigible [12].

As seen in Fig. 9, the air speed is increased on the rear of the propeller, which adds to the lift parameter. In particular, the simulation results show that the maximum air speed is ≈0.2 m/s in comparison with ≈0.02 m/s at the entrance of the propeller. After carrying out the simulations, we proceeded with the manufacturing of the gondola, the two propellers, and the rudder system (navigation control system).

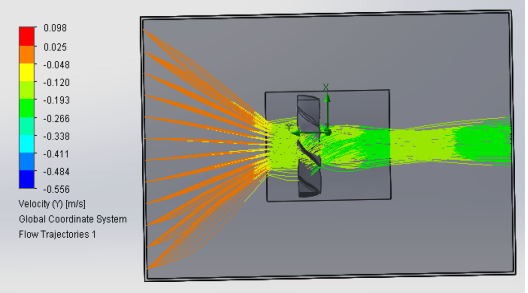

Figure 9. Propeller simulation [12].

V. Conclusions

In this paper, the simulation of a blimp kind UAV was shown. The design shown presents a mass of 0.917 kg, whereas the theoretical data establish a limit of 0.923 kg, meaning that the lift is on its limits. In this case, we pretended to reduce the mass of the electrical components using a custom Printed Circuit Board instead of using a globe with bigger dimensions. Actually, our team is currently working on an improved UAV design shown in Figs. 10–12. The design proposed does not modify the mass of the structure; however, the prototype will reduce the diverse external forces to increase the lift, drag, and thrust parameters.

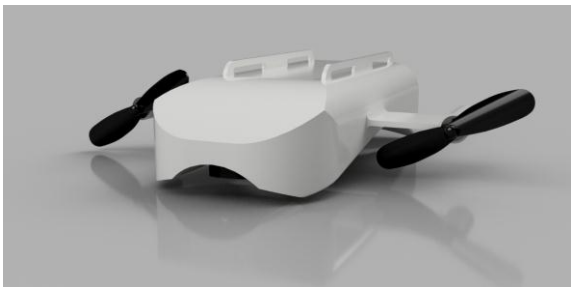

Figure 10. Improved gondola design (frontal view) [12].

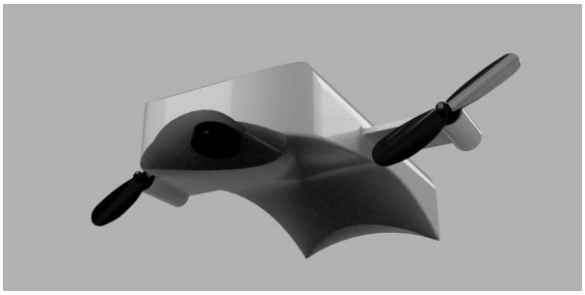

Figure 11. Improved gondola design (inferior view) [12].

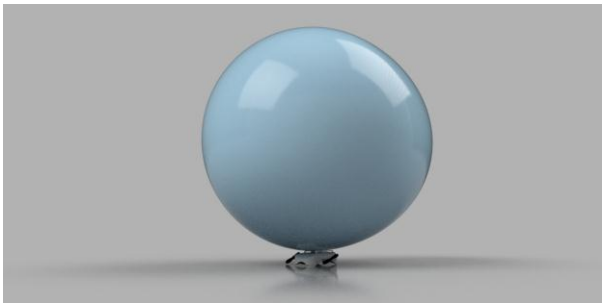

Figure 12. Improved overall system (gondola and globe) [12].

In addition, the simulation results provide important information about the differential wind speed in a particular section of the UAV to clarify the aerodynamic parameter performance. On the other hand, the results presented support the research and innovation regarding materials, structures, and new concepts for airframes for future aircraft to improve the aircraft performance parameters, such as vehicle weight, fuel consumption, noise, lift, drag, durability, and emissions, in particular for new low-density, high-strength fibers. Therefore, all of this allows innovation in processing methods to reduce the component manufacturing cost, mechanic design, and structural subcomponent design into system level designs. In general, although an aircraft can be of lighter-than-air (LTA) or heavier-than-air (HTA) kind, sometimes, the LTA type needs an extra aerodynamic analysis because of technical trade-offs. In our case, the prototype is in the LTA limit. Thus, an aircraft is modeled as a rigid body with three rotational and translational degrees of freedom (some shown in Figs. 5–9), which are represented by six differential equations; however, the obvious differences between HTA and LTA aircraft imply some specific modeling modifications. However, CAD and simulation allow rapid prototyping and modeling. In addition, wind-tunnel and flight tests are required to validate the simulation results.

Acknowledgements

We would like to thank E. Vargas for his important technical work [12], A. Pimentel, R. Ojeda-Arechiga, and J. Terrazas for the research and technical support during this project. The people mentioned worked hard in the same level as all the authors.

References

[1] S. Hayat, E. Yanmaz and R. Muzaffar, "Survey on unmanned aerial vehicle networks for civil applications: A communications viewpoint," *IEEE Communications Surveys & Tutorials*, vol. 18, no. 4, April 2016, pp. 2624 – 2661.

[2] T. Oliveira, A. P. Aguiar, and P. Encarnação, "Moving path following for unmanned aerial vehicles with applications to single and multiple target tracking problems," *IEEE Transactions on Robotics*, vol. 32, no. 5, 2016, pp. 1062-1078.

[3] K. J. Wu, T. S. Gregory, J. Moore, B. Hooper, D. Lewis, and Z. T. Ho-Tse, "Development of an indoor guidance system for unmanned aerial vehicles with power industry applications," *IET Radar, Sonar & Navigation*, vol. 11, no. 1, 2017, pp. 212-218.

[4] R. Montanari, D. C. Tozadore, E. S. Fraccaroli, and R. Romero, "Ground vehicle detection and classification by an unmanned aerial vehicle," in *Proc. 12th Latin American Robotics Symposium and 2015 3rd Brazilian Symposium on Robotics (LARS-SBR)*, 2015, pp. 253-258.

[5] D. Horvat, D. Kobale, J. Zorec, D. Mongus, and B. Žalik, "Assessing the usability of LiDAR processing methods on UAV data," *International Conference on Computational Science and Computational Intelligence (CSCI)*, 2016, pp. 665 – 670.

[6] D. C. Macke, S. E. Watkins, and T. Rehmeier, "Creative interdisciplinary UAV design," *IEEE Potentials*, vol. 33, no. 1, 2014, pp. 12-15.

[7] M. Liu, G. K. Egan, and F. Santoso, "Modeling, autopilot design, and field tuning of a UAV with minimum control surfaces," *IEEE Transactions on Control Systems Technology*, vol. 23, no. 6, 2015, pp. 2353-2360.

[8] H. Wang, Y. Wang, and M. Wang, "On the development of a landing gear design method in aircraft multidisciplinary design

environment," *IEEE International Conference on Aircraft Utility Systems (AUS)*, 2016, pp. 403-407.
[9] V. Srinivasa, G. A. Nagappa, S. Sridhara, and B.A. Biradar, "Estimation and reduction of drag in fuselage of solar powered UAV," *IEEE Aerospace Conference*, pp. 1-11, 2016.
[10] C. J. Salaan, Y. Okada, K. Hozumi, K. Ohno, and S. Tadokoro, "Improvement of UAV's flight performance by reducing the drag force of spherical shell," *IEEE/RSJ International Conference on Intelligent Robots and Systems (IROS)*, 2016, pp. 1708-1714.
[11] G. Atmeh and K. Subbarao, "Guidance, navigation and control of unmanned airships under time-varying wind for extended surveillance," *Aerospace*, vol. 3, no. 8; 2016, pp. 1-25.
[12] A.E. Vargas-Maldonado, "Diseño conceptual, análisis y simulación de una góndola para un vehículo aéreo no tripulado tipo dirigible",2016, CETYS University, Mexico.

J. A. López obtained his B.Sc. degree with an emphasis on telecommunications from the Cajeme Higher Institute of Technology (ITESCA) in Mexico. From 2006 to 2008, he worked on networking and telephony projects. Finally, he obtained his Ph.D. degree in quantum communication using satellites and quantum cryptography at the CICESE Research Center, Mexico, working together with Télécom ParisTech. His current research interests include free space optical communication in classical and quantum domains.

L. A. Aguilera is a Research Assistant at CETYS University, Mexico. In addition, he is a student of engineering in mechatronics and professional assistant for external technical projects.

M. Ponce received his B.Sc. degree in industrial physics engineering in 1987 from the Monterrey Institute of Technology and Higher Education. He is currently a Ph.D. candidate at the National Autonomous University of Mexico. His research interests include the design and manufacture of optomechanical devices, light-matter interaction, and biophotonic applications.

L. Basaca received his Ph.D. degree in optoelectronic analysis for position systems. Nowadays, he works in research lines such as robotics, control systems, and automation for the industrial sector.

R. I. Ramos Garcia received his B.Sc. degree in electronic engineering in 2007 from the Cajeme Higher Institute of Technology, Obregon City, Sonora, Mexico, and his Ph.D. degree in electrical engineering from Clemson University, Clemson, SC, USA, in 2014. He was a Postdoctoral Research Associate at the Computer Laboratory of Ambient and Wearable Systems (CLAWS) of the University of Alabama, Tuscaloosa, AL, USA. His research interests include machine learning, pattern recognition, signal processing, biomedical engineering, computer vision, speech processing, and embedded systems. He actually works in Phyn LLC Data Science and Machine Learning, WA.

V. M Ramos Garcia obtained his B.Sc. degree with an emphasis on industrial engineering from the Cajeme Higher Institute of Technology (ITESCA) in Mexico. Nowadays, he is Ph.D. student with research lines in optimized industrial processes based on technologies' trends.